

Adjoint modes as probes of gauge field structure

Antonio González-Arroyo and Robert Kirchner

18th November 2018

Depto. de Física Teórica C-XI
and
Instituto de Física Teórica UAM-CSIC
Universidad Autónoma de Madrid
Cantoblanco Madrid 28049 SPAIN

Abstract

We show how zero-modes and quasi-zero-modes of the Dirac operator in the adjoint representation can be used to construct an estimate of the action density distribution of a pure gauge field theory, which is less sensitive to the ultraviolet fluctuations of the field. This can be used to trace the topological structures present in the vacuum. The construction relies on the special properties satisfied by the supersymmetric zero-modes.

1 Introduction

The dynamics of gauge fields is expected to encompass some of the most fascinating phenomena, as confinement and chiral symmetry breaking, whose non-perturbative character makes them difficult to understand and describe. Lattice Gauge Theory has opened the way to a first principles calculational scheme of all the non-perturbative properties of the theory. In this way considerable evidence has accumulated over the years that Quantum Chromodynamics (QCD) does indeed possess this behavior. It is, nonetheless, important to know if it is possible to have a conceptually simpler description of these phenomena in terms of a restricted set of relevant degrees of freedom.

With the discovery of the instanton [1] and the subsequent qualitative solution of the $U_A(1)$ problem [2], giving the η' its mass by its coupling to the $U_A(1)$ current anomaly, it became clear that topology plays an important role in the low energy behavior of QCD. A longstanding question, which is still open, is whether the mechanism responsible for the spontaneous breakdown of chiral symmetry ($S\chi SB$) does involve topological configurations, with the instanton as fundamental structure. This point is connected with the more general one about the validity and usefulness of the semiclassical approach to describe this

and other non-perturbative aspects of QCD. In this respect a semiclassical picture of the vacuum was developed, the Instanton Liquid Model [3–5], which has met a certain degree of success in explaining some quantities. This picture provides a popular mechanism for the spontaneous breakdown of chiral symmetry, through the Banks-Casher relation [6], which relates the chiral condensate with the non-zero density of low-lying modes of the Dirac operator. The latter have its origin in the individual zero modes which the Atiyah Singer index theorem attributes to each instanton. In a dilute situation, with small overlap between neighboring instantons, these modes appear as quasi-zero modes contributing a finite density [7].

Although the mechanism is fairly appealing, there are several criticisms to the overall picture. For example, it has been suggested that the ILM as main mechanism for $S\chi SB$ is inconsistent with the expansion in the number of colors N . The argument is that at large N the instanton weight in the action is exponentially suppressed, while effects from quantum fluctuations decay according to $1/N$. This implies that at large N instantons are not likely to play a role in the breakdown of chiral symmetry, since their effect is washed out by quantum fluctuations. Therefore, according to this argument, either chiral symmetry is broken differently for large N than for $N = 3$, or $S\chi SB$ will not be caused by instantons in QCD. Another point of debate is the diluteness of the instanton vacuum. Other descriptions based on a more dense multi-instanton setting [8], might still inherit the same mechanism for $S\chi SB$ [9].

All these questions about the general role of topology and semiclassical methods in QCD should be resolved within the framework of lattice gauge theory. For this purpose different methods have been developed to extract the global and the local topology of lattice gauge fields in thermal equilibrium. The main problem one encounters in examining Monte Carlo generated lattice gauge field configurations, is that they are very rough, with sizable fluctuations at the scale of the lattice spacing. This *noise* dominates over the long wavelength signal one is willing to investigate. The roughness is to be expected, and is a reflection of the ultraviolet divergences of quantum field theory. Indeed, it is well known that even for a free field theory, continuous fields have zero-measure. In Quantum Mechanics the divergence is milder, but still differentiable paths have zero-measure. Thus, the rough *aura* of smooth gauge fields is essential in contributing sizably to the path integral. This, sometimes ignored fact, tells us that in the semiclassical approximation, smooth configurations act as labels to denote the finite probability regions centered around them.

A frequently used method to solve the aforementioned roughness problem is the so called *cooling* method [10,11]. Under this generic term a number of different procedures have been developed, which have in common that they produce a sequence of increasingly smooth configurations by locally minimizing the action. Ideally, the method should produce the smooth *labelling* configuration associated to the rough initial one. However, if cooling is applied indefinitely one would reach a relative minimum of the action, in which most of the local information would be lost. Thus, beyond being useful in determining global topological quantities as the topological susceptibility [12], its validity to deter-

mine the local topology of the field, has been heavily and severely criticized. Nevertheless, we think that cooling is indeed a useful method when used judiciously and in certain situations. The main issue has to do with a hierarchy in the variations of the action within the space of gauge field deformations. We know that variations associated to rough fields produce large changes in the action. On the other hand, there is sometimes a subclass of smooth gauge fields configurations associated to “almost flat” directions. This is indeed the case in a dilute instanton gas situation, for example. This hierarchy then would translate into an equivalent hierarchy of “cooling time” scales. Thus, when cooling is applied, movement in the steeper directions happens relatively fast, while that along the “almost flat” directions is much slower. In addition, since cooling is a local algorithm, the evolution of large momenta components starts earlier. In any case, the usefulness of the semiclassical approach depends also on the observable being studied. As in every reduced degrees of freedom approach, a la Ginzburg-Landau, the projected degrees of freedom have to capture the essence of the physics being studied. Accordingly, if physical results have to be extracted from cooling, they should be independent of the number of cooling steps applied within a certain window, or change in a prescribed and computable fashion.

A different approach to disentangle the local topological structure of the lattice field, is commonly referred to as smoothing. It is a local procedure which substitutes a link with a weighted average of link paths. The prototype of smearing is APE-smearing [13], but as in the case of cooling there is a number of algorithms in use, which however all share the common feature of averaging in some sense the gauge field locally. As in the case of cooling, smearing has successfully been used in determining the topological susceptibility [14–17], but has been the object of criticism when local topological questions are concerned. It is frequently stated that from a conceptual point of view smoothing is preferable over cooling, since the continuum limit of the gauge field is not changed in the process. However, as in the case of cooling, an indefinite number of steps would end up washing out all local structures. Therefore, similar considerations as before are necessary.

A more recent proposal to study vacuum topology uses fermionic degrees of freedom. Introduced some time ago [18], fermionic methods rely on their response to the background gauge field. They suffer from the traditional problems associated to the breaking of chiral symmetry on the lattice. With the discovery that lattice Dirac operators which satisfy the Ginsparg-Wilson relation, as in the domain Wall formulation [19–21] or the overlap operator [22, 23], possess a lattice remnant of chiral symmetry at finite lattice spacing and satisfy exact index theorems, fermionic methods have become fully applicable. In various works [24–33] these methods have been used to investigate the question of the local topological structure of the QCD vacuum. It is argued that an instanton dominated vacuum will lead to a spectrum of low-lying eigenmodes of the Dirac operator, which originates from the mixing of the zero-modes each instanton would contribute if it were isolated. The local chirality of the near zero-modes is then used as a measure of the topological origin of the mode. It has been found [24, 25, 27, 28, 34] that the local chiral structure of the low-lying

modes of the Dirac operator does not exclude the ILM as a microscopically accurate picture of the vacuum. However, it is still a matter of debate whether the structure of local chirality found in the low-lying modes does indeed have a topological origin closely related to instantons or follows from other structures [29, 31–33, 35, 36].

In the present work we want to propose a new method to investigate the local topological structure of the gauge fields, which is a hybrid of the above. It adheres to the idea of using fermionic quasi-zero-modes to investigate the underlying local topology of the configurations. However, in our proposal we use the Dirac operator in the adjoint representation. One of the advantages of using adjoint zero-modes instead of fundamental ones is that some of these modes do exactly mimic the structure of the action density for classical solutions of the equations of motion. These particular modes are the supersymmetric partners of the corresponding gauge fields. They possess a peculiar reality property which allows to distinguish them from other modes. Thus, for gauge field configurations which are classical solutions of the equations of motion, we can construct two functions S_{\pm} which reproduce the shape of the self-dual and anti-self-dual parts (respectively) of the action density up to an overall normalization. Following the same reasoning as in [29, 37], for a smooth background gauge field which is “almost” self-dual (as for example a configuration consisting of dilute (anti)instantons) we expect to find an “almost” supersymmetric solution from which we can reconstruct the form of the underlying gauge field.

The main usefulness of this idea arises in the presence of quantum fluctuations. The quantities S_{\pm} are less sensitive to the ultraviolet modes than the action density itself. This follows from the non-local (extended) nature of these observables. Thus, as we will see, it is still possible to reconstruct the long wavelength features of the configuration and its topological structure in the presence of quantum fluctuations of limited size. This paper is devoted to presenting the observables, the numerical method and to displaying its behavior for smooth configurations, as well as in the presence of controlled quantum fluctuations. A detailed analysis of Monte Carlo generated configurations is deferred to later works. For that, it is desirable to use a chiral invariant lattice Dirac operator, as the overlap. In the present paper we have used Wilson fermions and our results indicate that even in the worst cases studied, the new observables seem to extract the local topology of the configuration after a very small (1-3) number of cooling steps are applied.

The paper is organized as follows: In Section 2 we review the main continuum formulas concerning the low-lying eigenstates of the massless adjoint Dirac operator (adjoint modes), on which our numerical method is based. First, we discuss the situation for solutions of the classical equations of motion. We identify the supersymmetric zero-modes and discuss their properties. We then study the behavior of the observables for configurations in the vicinity of a solution. In Section 3 we discuss the lattice setup, i.e. the operators, the algorithms and the configurations used throughout our work. We also introduce the numerical method which we use to project onto the supersymmetric or the “almost” supersymmetric solution of the Dirac operator in a given background field. In Section

4 we apply the method to specific configurations in order to explore its ability to reconstruct the form of the underlying gauge field. We start by considering (anti)self-dual configurations and we show how our numerical method is capable of isolating the supersymmetric solution, and how we can, with a high degree of accuracy, reconstruct the shape of the action density from these solutions. We then proceed with more complex smooth fields such as the non self-dual case of an instanton anti-instanton pair. Finally we introduce quantum fluctuations. This we do by applying a given number of *heating* Monte Carlo steps to an initial one-instanton configuration. For large β and a small number of cooling steps we have control that the underlying topological structure of the configuration is unchanged and we can check the ability of our observables to reconstruct it. We also present results for smaller values of β . Here, the quantum fluctuations can change the long wavelength structure of the configuration, so our method is then used in conjunction with cooling and smearing. Results are promising, but we believe a more accurate analysis has to be done employing a chiral invariant lattice Dirac operator. Finally, in Section 6 we will summarize our conclusions.

2 Adjoint modes of the Dirac Operator

In this section we will shortly revise the main formulas and explain the philosophy of our method in the continuum. We will be using the notation collected in the Appendix. Let us consider smooth SU(N) Yang-Mills field configurations on 4-dimensional euclidean space-time. Although the topology of space-time is not essential for the construction, in order to explain the numerical applications on the lattice, we will take space-time to be given by a 4-dimensional torus. Gauge fields are then connections on a (SU(N)) bundle over the torus; the latter are classified into topologically inequivalent classes determined by the twist sectors $n_{\mu\nu}$ and the instanton number $Q = \frac{(N-1)}{4N}n_{\mu\nu}\tilde{n}_{\mu\nu} + q$, where q is an integer [38, 39]¹. It is customary to split the antisymmetric integer-valued twist tensor $n_{\mu\nu}$ into its spatial ($m_i = \frac{1}{2}\epsilon_{ijk}n_{jk}$), and temporal ($k_i = n_{0i}$) components. In this form the instanton number reads

$$Q = q + \left(\frac{N-1}{N}\right)\vec{k} \cdot \vec{m}, \quad q \in Z \quad (1)$$

Notice that the instanton number is not necessarily an integer since $\frac{1}{4}n_{\mu\nu}\tilde{n}_{\mu\nu} = \vec{k} \cdot \vec{m}$ need not be a multiple of N .

We will now consider spinor fields $\Psi(x)$ transforming in the adjoint representation of the gauge group. One can study the spectrum of the Dirac operator in the background of the gauge field configuration:

$$\mathcal{D}^A \Psi^{(\lambda)} = i\lambda \Psi^{(\lambda)} \quad (2)$$

¹In the mathematical literature for SU(2) these are associated to Stiefel-Whitney and Chern classes respectively. The reader is referred to Ref. [40] for a mathematically rigorous introduction to the subject.

The eigenvalues $i\lambda$ are (at least) twice degenerate as a consequence of (euclidean space) charge conjugation symmetry, which follows from the reality of the adjoint covariant derivative. Thus, for any solution $\Psi^{(\lambda)}$ of Eq. 2 we can construct a new one as follows:

$$\Psi_c^{(\lambda)} \longrightarrow \gamma_5 C \Psi^{(\lambda)*} \quad (3)$$

where $*$ denotes complex conjugation. This can be easily proven by complex conjugating Eq. 2. The new solution is orthogonal to the previous one (this follows from the antisymmetry of C).

The positive and negative values of λ are exactly mapped onto each other by multiplying the eigenvector by γ_5 . In addition, there might be zero-modes ($\lambda = 0$). The Atiyah-Singer index theorem expresses the index of the Dirac operator (number of zero-modes of positive chirality minus the number of zero-modes of negative chirality) in terms of the instanton number:

$$\text{index } \mathcal{D}^A = 2N Q \quad (4)$$

Notice that although Q need not be an integer, the index is always an even number. As a matter of fact, in the presence of non-zero twist ($\vec{k}, \vec{m} \neq 0$), the gauge group is $SU(N)/Z(N)$ and the topological charge should be computed in the adjoint representation, which a faithful representation of this group. Then, the topological charge becomes precisely equal to the integer $2NQ$. It is easy to understand the evenness as due to the two-fold degeneracy mentioned previously, which affects zero-modes of each chirality.

The positive and negative chirality zero-modes (ψ_{\pm}) satisfy the following Weyl equations:

$$\bar{D}^A \psi_+ = 0 \quad (5)$$

$$\hat{D}^A \psi_- = 0 \quad (6)$$

respectively. Contrary to the situation for zero-modes of the Dirac operator in the fundamental representation, the shape of adjoint zero-modes is in some cases directly expressible in terms of the action density of the gauge field. In particular, suppose that A_{μ} is a gauge field configuration which is a solution of the euclidean equations of motion (not necessarily self-dual or anti-self-dual), then the following four-spinor:

$$\Psi^a(V, x) = \frac{1}{8} \mathbf{F}_{\mu\nu}^a(x) [\gamma_{\mu}, \gamma_{\nu}] V \quad (7)$$

is an adjoint zero-mode for any constant four-spinor V [41, 42]. This provides, if non-zero, two linearly independent positive chirality $\Psi_+^a(x)$ and two negative chirality $\Psi_-^a(x)$ zero modes. The gauge invariant densities $|\Psi_{\pm}^a(x)|^2$ are equal (with the normalization given in Eq. (7) and unitary V) to the self-dual/anti-self-dual parts of the action density respectively. This is the crucial result that we are using in what follows. Since, the spinor field Eq. 7 can be obtained by applying a supersymmetry transformation to the gauge fields, we will refer to it by the term ‘‘supersymmetric zero-mode’’.

There is an interesting property satisfied by $\Psi_{\pm}^a(V, x)$ which will allow us to single it out when there are several zero-modes present. To explain it, it is better to take the chiral representation for the Dirac matrices given in appendix A. Choosing $V^{\dagger} = (1 \ 0 \ 0 \ 0)$ one gets an adjoint zero-mode of positive chirality such that the real part of the first spinor component of $\Re(\Psi^{a+}(V, x))$ vanishes in every space-time point, for any value of the color index and all components in color-space. Explicitly this positive chirality solution takes the form:

$$\Psi_+^a = i \begin{pmatrix} \frac{(B_3^a + E_3^a)}{2} \\ \frac{(B_1^a + E_1^a)}{2} - i \frac{(B_2^a + E_2^a)}{2} \\ 0 \\ 0 \end{pmatrix}. \quad (8)$$

For $V^{\dagger} = (0 \ 1 \ 0 \ 0)$ the positive chirality solution $(\Psi_+^a)_c = \gamma_5 C(\Psi_+^a)^*$ is found. In case of a self-dual gauge field, electric and magnetic field components coincide: $\vec{B}^a = \vec{E}^a$. The reality property of this zero-mode is non-trivial: for a generic solution it cannot be implemented by simply performing a gauge transformation or taking an appropriate choice of V . The negative chirality solutions can be worked out analogously, and the same conclusion follows.

We have investigated whether the reality property is shared by other zero-modes. In the simplest case of a single SU(2) instanton we have 4 positive chirality adjoint zero-modes, grouped in two charge-conjugate pairs. One of the pairs is the one corresponding to Eq. (7), and the other does not satisfy the property. We have also investigated the general ADHM [43] case, which expresses adjoint zero-modes in terms of the ADHM data. Except in exceptional limits, this property only takes place for this special zero-mode.

After this preamble we will now explain the philosophy of our method. Consider the case of a general gauge field configuration, not necessarily an exact solution of the euclidean classical equations of motion. Our strategy is to define a preferred spinor field in each chirality sector (a preferred section). The corresponding densities give rise to two positive definite functions of space-time S_{\pm} . Their structure will trace that of the gauge field from which they are constructed. We will exploit the previous considerations by requiring that for gauge fields which are solutions of the classical equations of motion these quantities S_{\pm} will coincide with the supersymmetric mode densities mentioned previously. Thus, they will be directly proportional to the self-dual or anti-self-dual parts of the action density (for left and right chiralities respectively). However, the main advantage of our observables compared to the action densities themselves appears when considering configurations containing quantum fluctuations. Our observables will be better behaved in the ultraviolet.

There can be several ways to make the choice of section in order to implement the program. It is at present unclear to us if there is an optimal choice. A particular simple and elegant possibility is to take as preferred section the eigenfunction of lowest eigenvalue (ground state) of the positive-hermitian operators O_{\pm} , given by the restrictions of $-D\bar{D}$ (for left spinors) and $-\bar{D}D$ (for right spinors) to the space of states satisfying the reality condition. These op-

erators can be rewritten as real symmetric operators acting on the space of real three-component functions as follows:

$$(O_{\pm})_{ij}^{ab} = \Delta^{ab} \delta_{ij} \pm 4F_k^{\pm c} \epsilon_{ikj} f_{acb} \quad (9)$$

where Δ^{ab} is the covariant laplacian in the adjoint representation and $F_k^{\pm c} = \frac{1}{2}(E_k^c \pm B_k^c)$. The indices a, b, c represent color in the adjoint representation and i, j, k run from 1 to 3.

The considerations made earlier in this section show that for a classical solution of the euclidean equations of motion, $O_{\pm}^{(0)}$ has a non-degenerate ground state with vanishing eigenvalue, and the densities S_{\pm} are the self-dual and anti-self-dual action densities. If we now perturb the gauge field configuration, it is clear that the non-degeneracy of the ground state is preserved for small enough deformations. One can use perturbation theory to compute the structure of the ground state in this case. The variation of the ground state (and its density) does not agree with the variation of the action density. Instead, it is expressed in terms of the Green function of the operator $O_{\pm}^{(0)}$. This a non-local expression which suppresses the small wavelength fluctuations with respect to the large wavelength ones. This is the effect we were looking for.

For technical reasons, related to the availability of code and data, in the numerical part of this paper we have chosen a definition of the densities which is slightly different from the one presented in the previous paragraph. Rather than imposing reality and looking for the ground states of O_{\pm} , we have searched within the space of low lying modes of the Dirac operator, those which best satisfy the reality condition. This is a change of order of the basic ingredients which, as we will see in the following sections, also gives rise to the required behavior.

3 Lattice Methods

3.1 Lattice Dirac operator

In order to translate the above procedure to the lattice, a suitable discretization of the adjoint Dirac operator has to be adopted. For this pilot study we have chosen Wilson discretization in the adjoint representation:

$$\begin{aligned} (D_W)_{ab}^{\alpha\beta}(x, y) &= 4r\delta_{ab}\delta_{xy}\delta^{\alpha\beta} \\ &- \frac{1}{2} \sum_{\mu=1}^4 [\delta_{y, x+\hat{\mu}}(r + \gamma_{\mu})^{\alpha\beta} V_{\mu, ab}(x) \\ &+ \delta_{y+\hat{\mu}, x}(r - \gamma_{\mu})^{\alpha\beta} (V^T)_{\mu, ab}(y)], \end{aligned} \quad (10)$$

where $V_{\mu, ab}(x)$ is the link in the adjoint representation of the gauge group (see the Appendix, Eq. (18)).

The above operator has the following properties:

$$\begin{aligned} C^{-1}D_W C &= D_W^T, \\ \gamma_5 D_W^\dagger \gamma_5 &= D_W, \end{aligned}$$

which implies that $(\gamma_5 D_W)$ is hermitian.

For our numerical work we will consider the eigenstates of the positive operator $(\gamma_5 D_W)^2$. Because of the symmetry properties described by Eq. (3) the eigenspaces are (at least) two-fold degenerate.

Let us comment on the eigenvalue structure of $(\gamma_5 D_W)^2$ for self-dual or anti self-dual background fields. From the Atiyah-Singer index theorem we know that for a massless continuum Dirac operator in the adjoint representation of the gauge group, and in the background of a $SU(N)$ gauge field carrying charge Q , we will find $\text{Index}(\mathcal{D}) = 2N|Q|$ zero-modes, with definite chirality. On the lattice, using $(\gamma_5 D_W)^2$ as Dirac operator, this translates to finding $2N|Q|$ eigenvectors with “small” eigenvalues and given chirality. These “small” eigenvalues are separated by a gap from a more densely populated band. In what follows we will refer to the modes with small eigenvalues in the above sense as approximate zero-modes.

Another important point concerns the chiral properties of the Wilson-Dirac operator. The explicit breaking of chiral symmetry by this operator might pose a problem, since the properties of the eigenmodes of the Dirac operator we wish to study on the lattice depend very much on chirality. The smaller the value of the parameter r , the smaller is the breaking of naive chirality. However, this conflicts with the splitting given to the doublers. Our final choice has been to work at the small value $r = 0.3$ of the Wilson parameter. As we will verify a posteriori this choice is small enough so that the properties we wish to study that depend on chirality are not too seriously affected. To check that there is no sizeable contamination of doublers in the low edge of the spectrum that we study, we computed the matrix elements in the corresponding eigenspace of the Wilson operator, defined by:

$$\begin{aligned} (W)_{ab}^{\alpha\beta}(x, y) &= 4\delta_{ab}\delta_{xy}\delta^{\alpha\beta} \\ &- \frac{1}{2} \sum_{\mu=1}^4 [\delta_{y, x+\hat{\mu}} \delta^{\alpha\beta} V_{\mu, ab}(x) \\ &+ \delta_{y+\hat{\mu}, x} \delta^{\alpha\beta} (V^T)_{\mu, ab}(y)], \end{aligned} \tag{11}$$

This procedure has been used previously by our group and is known to work well for smooth gauge field configurations. For rough, Monte Carlo generated configurations it is certainly desirable to use a discretization which is more respectful of chiral symmetry, such as the Neuberger operator [22, 23]. Nevertheless, for the sake of our paper we concluded that the much less computationally costly Wilson-Dirac operator still allowed us to exemplify the validity of our idea.

3.2 Projecting onto the supersymmetric solution

In Section 2 we have defined our procedure in the continuum. Our goal is to construct two positive functions of space S_{\pm} for each gauge field configuration. For the case that the gauge field is a solution of the Euclidean equations of motion S_{\pm} they reproduce exactly the shape of the self-dual and anti-self-dual parts of the action density. Deforming away from them, we have argued that these quantities are less sensitive to the ultraviolet modes of the gauge field than the action density itself. Thus, in the presence of quantum fluctuations they produce an estimate of the long-range topological structure of the configurations. To provide a lattice implementation, let us first consider the case in which the link variables are a lattice discretization of a background gauge field which is a solution of the classical Euclidean equations of motion having a non-trivial self-dual part. In this case we first have to look at the low-lying eigenstates of the Wilson-Dirac operator. This space of states should contain the discretized zero-modes. We then explore within this space to find the state that best projects onto the positive chirality supersymmetric solution Eq.(8) of the Weyl equation. To single out this solution we make use of the reality property of the cuadrspinor of Eq.(7) discussed in Section 2. On the lattice this is done by looking at the linear combination of approximate zero-modes that has minimal imaginary part of the first spinor component for all colors and at each point of space-time. We also require that the solution is as chiral as possible. If we indicate by ϕ_i the elements of the set of linearly independent quasi-zero modes, then our solution can be written as

$$\Psi_+ = \lambda_i \phi_i \quad (12)$$

The coefficients λ_i are chosen such that

$$c = \sum_{x,a} (\text{Im}\Psi_+^{1,a}(x))^2 + \sum_{x,a,s=3,4} (\text{Re}\Psi_+^{s,a}(x))^2 + (\text{Im}\Psi_+^{s,a}(x))^2 \quad (13)$$

is minimal.

In the same way, for a field having a non-trivial anti self-dual part, the negative chirality solution Ψ_- corresponding to Eq.(8) in the continuum, can be calculated by minimizing in Eq.(12) the imaginary part of the third component and the first and second component (chirality).

In terms of the coefficients λ_i Eq. (13) can be written as a quadratic form:

$$c = \langle v, Mv \rangle, \quad \text{with} \quad v = \begin{pmatrix} \text{Re}\lambda_i \\ \text{Im}\lambda_i \end{pmatrix}, \quad M = \begin{pmatrix} A & B \\ B^T & C \end{pmatrix}. \quad (14)$$

The matrix M is $2n$ dimensional, where n is the number of eigenstates of the Dirac operator among which the minimization is carried out. It is straightfor-

ward to work out the detailed form of the sub-matrices A, B and C:

$$\begin{aligned}
A_{k,l} &= \sum_{x,a} \text{Im}\phi_k^1 \text{Im}\phi_l^1 + \sum_{x,a,s=3,4} \text{Im}\phi_k^s \text{Im}\phi_l^s + \text{Re}\phi_k^s \text{Re}\phi_l^s, \\
B_{k,l} &= \sum_{x,a} \text{Im}\phi_k^1 \text{Re}\phi_l^1 + \sum_{x,a,s=3,4} \text{Im}\phi_k^s \text{Re}\phi_l^s - \text{Re}\phi_k^s \text{Im}\phi_l^s, \\
C_{k,l} &= \sum_{x,a} \text{Re}\phi_k^1 \text{Re}\phi_l^1 + \sum_{x,a,s=3,4} \text{Re}\phi_k^s \text{Re}\phi_l^s + \text{Im}\phi_k^s \text{Im}\phi_l^s,
\end{aligned}$$

M is also hermitian, positive, and for normalized vectors v the minimal eigenvalue of M is the minimum of expression (13). The corresponding eigenvector v provides the real and imaginary part of the coefficients λ_i .² The lattice approximation Ψ_{\pm} to the supersymmetric solution can be obtained by using to Eq.(12) with the λ_i obtained in the previous procedure.

Then, $S_{\pm}(x)$ are then defined as:

$$S_+(x) = \langle (\Psi_+)_L, (\Psi_+)_L \rangle, \quad S_-(x) = \langle (\Psi_-)_R, (\Psi_-)_R \rangle. \quad (15)$$

where brackets denote scalar products in spinor and color space. Note that since the reality property is very restrictive, finding the vector that minimizes expression (13) in a larger space containing all approximate zero modes, will, up to numerical errors, not influence result. This is crucial, since one does not know how many zero-modes one should find for a generic gauge field. This observation will also play a role later in testing the applicability and stability of the above described numerical procedure.

3.3 Technicalities

Let us briefly mention some technical details of this work. For the numerical part we used $SU(2)$ configurations throughout. The self-dual gauge configurations have in all cases been obtained by standard cooling [10,11].

Next to cooling we also use APE-smearing [13] to smoothen the configurations in some cases. The N^{th} -level APE-smear link with smearing parameter c is defined as:

$$\overline{U}_{\mu}^{(i)}(x) = (1-c)U_{\mu}^{(i-1)}(x) + \frac{c}{6} \sum_{\substack{\alpha=\pm 1 \\ |\alpha| \neq \mu}}^{\pm 4} U_{\alpha}^{(i-1)}(x) U_{\mu}^{(i-1)}(x + \hat{\alpha}) U_{\alpha}^{(i-1)}(x + \hat{\mu})^{\dagger},$$

with $\overline{U}_{\mu}^{(i)}(x)$ projected back in $SU(2)$ after each smearing step. For small smearing parameter c this corresponds to a diffusion process with a diffusion radius:

$$R_s = Nc.$$

To introduce short range ultraviolet fluctuations the heat-bath algorithm of [47] was used. The lattice action used is the usual Wilson action. The topological

²The complete diagonalization of M can be carried out by standard libraries.

charge operator we use to identify the charge of smooth gauge field configurations is the field theoretic operator discussed in [46]. The low-lying eigenstates and their respective eigenvalues of the operator ($\gamma_5 D_W$) are calculated with the conjugate gradient algorithm proposed by Kalkreuther and Simma [44], and with the implicitly restarted Arnoldi algorithm [45]. For lattice sizes 8^4 , 12^4 and $12^3 * 24$ we computed about 10 to 20 eigenstates.

4 Results

In this section we will present the results obtained by applying the numerical procedure of projecting onto the supersymmetric modes of the adjoint Dirac operator described in the previous sections. We will consider certain SU(2) gauge configurations on the lattice in an increasing order of complexity. First we investigate the case of smooth (anti)self-dual configurations. This will test the efficiency of our method to identify the supersymmetric zero-mode Eq. (8) within the subspace of low-lying eigenstates. The situation becomes more difficult the larger the value of the topological charge $|Q|$, since the dimensionality of the zero-mode manifold ($4|Q|$) increases.

After, we will also apply the procedure to smooth configurations which are not solutions of the classical equations of motion, and in particular the case of an instanton anti-instanton pair. Thus, the solution will not be an exact zero-mode of the Dirac operator anymore. Finally, we will conclude by adding quantum fluctuations to the gauge field configurations. This is done by subjecting them to a given number of Monte Carlo updating steps.

4.1 Smooth self-dual Configurations

We begin by applying our procedure to obtain the supersymmetric zero-mode of the adjoint Dirac operator for a number of (anti)self-dual configurations with increasing values of the topological charge $|Q|$ (see Table 1). The smallest absolute value of topological charge we consider is $Q = -\frac{1}{2}$, which demands the use of twisted boundary conditions ($\langle m, k \rangle \neq 0$) as explained in section 2.

lattice: L, T	$S/(8\pi^2)$	Q_L	Twist _m	Twist _k	r	#Eigenst.
8,8	0.493	-0.47	1 1 1	1 1 1	0.3	10
12,12	1.02	-0.90	0 0 0	0 0 0	0.3	16
12,12	1.51	-1.41	1 1 1	1 1 1	0.3	16
12,12	1.97	1.86	1 0 1	0 1 0	0.3	20

Table 1: *Configurations for which the reconstruction of the supersymmetric zero-mode was carried out. The values of Q_L were obtained with the field-theoretic unsmearred topological charge operator. The second column gives the total action S divided by $8\pi^2$.*

1. $Q = -\frac{1}{2}$, $\mathbf{m}=\{111\}$, $\mathbf{k}=\{111\}$

In the case of an anti self-dual $Q = -\frac{1}{2}$ field there are only two zero-modes which correspond to the supersymmetric solution Eq. (8). We have numerically calculated the ten lowest-lying modes of the operator $(\gamma_5 D_W)^2$ in this background. The results are summarized in Table 2. Notice that the eigenvalues are twice degenerate as follows from the symmetry $\phi_i = \gamma_5 C^{-1} \phi_{i+1}^*$ (see section 2). In the Table we also show the chirality $(\langle \phi, \gamma_5 \phi \rangle)$ of each mode.

Eigenvalue	$\langle \phi, \gamma_5 \phi \rangle$
$\lambda_1=2.44 * 10^{-3}$	-0.998
$\lambda_3=2.68 * 10^{-1}$	0.108
$\lambda_5=2.68 * 10^{-1}$	0.108
$\lambda_7=2.68 * 10^{-1}$	0.108
$\lambda_9=2.93 * 10^{-1}$	-0.106

Table 2: *Lowest eigenvalues of the operator $(\gamma_5 D_W)^2$, and the chirality of the corresponding modes, for the configuration with $Q = -\frac{1}{2}$.*

There is a clear gap of two orders of magnitude between the first two eigenvalues and the higher states. Accordingly, we can identify the modes pertaining to $\lambda_{1,2}$ with the zero-modes. This is also clear from the chirality of the modes. To confirm that their structure is the one given by Eq.(8), we compare the chiral density

$$\langle \Psi_R, \Psi_R \rangle \propto_{a \rightarrow 0} \text{Tr}[F_{\mu\nu} F_{\mu\nu}] + O(a^2), \quad (16)$$

of the lowest lying mode with the action density. The shapes are displayed in Figure 1 for a given plane, and show a nice match up to an overall normalization. The latter might be fixed by the value of the topological charge alone.

It is important to test the stability of the method with respect to the number of eigenmodes considered, since ultimately one wants to apply the method to situations for which the number of quasi-zero modes is not determined a priori. For that purpose, we have considered the full space of ten eigenmodes and applied the minimization condition (13) to the matrix M (see Section 3.2). The vector that achieves the minimum is indeed dominated by the two low-lying modes, with the remaining modes giving contributions two orders of magnitude smaller. The density profile is only slightly changed.

2. $Q = -1$, $\mathbf{m}=\mathbf{k}=\{000\}$

For an anti self-dual $Q = -1$ configuration the space of zero-modes is

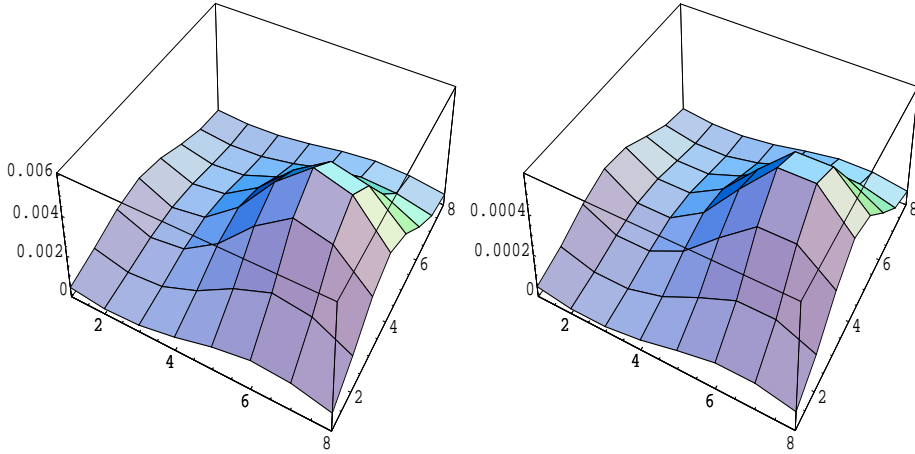


Figure 1: Action density F^2 (left) and chiral density $\langle \Psi_R, \Psi_R \rangle$ (right) along a t - z plane, for the configuration with $Q = -\frac{1}{2}$.

four dimensional. To find the zero-mode of Eq. (8) we have calculated the sixteen lowest-lying eigenstates of $(\gamma_5 D_W)^2$ in this background. The results are shown in Table 3. We find four small eigenvalues which are separated by one order of magnitude from the higher ones. The corresponding eigenvectors have definite chirality, and we identify these modes as the zero-modes predicted in the continuum by the Atiyah-Singer index theorem. In principle the solution (8) that we are looking for is a linear

Eigenvalue	$\langle \phi, \gamma_5 \phi \rangle$	Eigenvalue	$\langle \phi, \gamma_5 \phi \rangle$
$\lambda_1 = 7.79 * 10^{-5}$	-0.997	$\lambda_9 = 5.11 * 10^{-2}$	0.057
$\lambda_3 = 7.40 * 10^{-3}$	-0.976	$\lambda_{11} = 5.34 * 10^{-2}$	-0.057
$\lambda_5 = 1.35 * 10^{-2}$	$0.178 * 10^{-2}$	$\lambda_{13} = 7.49 * 10^{-2}$	0.067
$\lambda_7 = 2.25 * 10^{-2}$	$-0.164 * 10^{-2}$	$\lambda_{15} = 8.41 * 10^{-2}$	-0.075

Table 3: Lowest eigenvalues of the operator $(\gamma_5 D_W)^2$ and chiralities of the respective eigenstates, for the configuration with $Q = -1$.

combination in the space of these zero-modes. Applying the minimization within this four dimensional space, we indeed find that the minimizing vector Ψ_- has the expected structure given by Eq. (8). We exhibit this by plotting the chiral density (16) in a fixed plane and comparing it to the action density in the same plane (see Figure 2). Including in the minimization all eigenstates that we have calculated, the same linear combination is selected (new coefficients are suppressed by two orders of magnitude) as in the space of zero-modes. Accordingly, also in the case of $Q = -1$ we

obtain stable results.

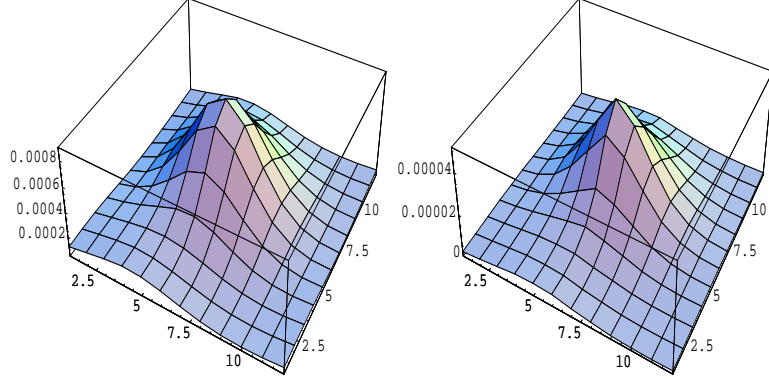


Figure 2: *Action (left) and chiral (right) densities for the $Q = -1$ configuration, for a given t - z plane.*

3. $Q = -1.5$, $\mathbf{m}=\{\mathbf{111}\}$, $\mathbf{k}=\{\mathbf{111}\}$

In the case of the $Q = -1.5$ configuration we find 6 low-lying modes that are divided by a gap of about two orders of magnitude from a band of higher eigenvalues (see Table 4). Again we find by minimizing expression (13) in the space of these lowest lying modes that the resulting linear combination is of the form of Eq. (8) (see Figure 3). Including all higher eigenmodes in the minimization does not change the linear combination appreciably, and hence, also in this case the minimization is stable.

Eigenvalue	$\langle \phi, \gamma_5 \phi \rangle$	Eigenvalue	$\langle \phi, \gamma_5 \phi \rangle$
$\lambda_1=9.00 * 10^{-4}$	-0.997	$\lambda_9=1.16 * 10^{-1}$	-0.085
$\lambda_3=1.38 * 10^{-3}$	-0.995	$\lambda_{11}=1.23 * 10^{-1}$	0.086
$\lambda_5=3.25 * 10^{-3}$	-0.990	$\lambda_{13}=1.32 * 10^{-1}$	0.077
$\lambda_7=1.05 * 10^{-1}$	0.090	$\lambda_{15} = 1.36 * 10^{-1}$	-0.082

Table 4: *Lowest lying eigenvalues of the operator $(\gamma_5 D_W)^2$ and chiralities of the respective eigenstate, for the configuration with charge $Q = -\frac{3}{2}$.*

4. $Q = 2$, $\mathbf{m}=\{\mathbf{101}\}$, $\mathbf{k}=\{\mathbf{010}\}$

The next case we consider in order to test our method is $Q = 2$. We find eight low-lying modes (see Table 5) which are divided by an order of magnitude from the higher eigenvalues. As above, minimizing Eq. (13) selects the wave function Eq. (8) among the eight lowest lying modes which

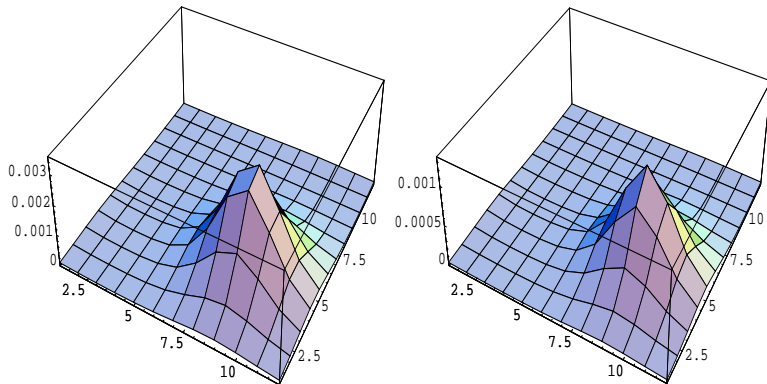


Figure 3: *Action (left) and chiral density (right) for the $Q = -1.5$ configuration; both in the t, z plane.*

we associate to the zero-modes of the continuum configuration (see Figure 4). As in all other cases we observe stability of the projection onto the supersymmetric mode when the higher modes are included.

Eigenvalue	$\langle \phi, \gamma_5 \phi \rangle$	Eigenvalue	$\langle \phi, \gamma_5 \phi \rangle$
$\lambda_1 = 6.28 * 10^{-4}$	0.997	$\lambda_{11} = 8.87 * 10^{-2}$	0.090
$\lambda_3 = 1.20 * 10^{-3}$	0.995	$\lambda_{13} = 1.02 * 10^{-2}$	-0.085
$\lambda_5 = 1.98 * 10^{-3}$	0.991	$\lambda_{15} = 1.14 * 10^{-2}$	0.084
$\lambda_7 = 7.27 * 10^{-3}$	0.982	$\lambda_{17} = 1.21 * 10^{-2}$	-0.085
$\lambda_9 = 7.50 * 10^{-2}$	-0.094	$\lambda_{19} = 1.30 * 10^{-2}$	-0.080

Table 5: *Lowest lying eigenvalues of the operator $(\gamma_5 D_W)^2$ and chiralities of the respective eigenstate, for the configuration with $Q = 2$.*

If a (anti-)self-dual configuration consists of well separated instantons or anti-instantons, a new complication can arise. In the continuum, as the separation becomes infinite, the zero-modes tend to those of isolated instantons, one of which will satisfy the reality condition. This is one of the limiting cases that we mentioned before for which there is more than one zero-mode satisfying the reality condition. It is clear that the chiral density of all states in this subspace of real zero-modes reproduces the sum of the action density of all the instantons weighted in various ways. As the instantons approach, the reality only remains true for a single (charge conjugate pair) eigenmode weighting all instantons equally: the supersymmetric zero-mode. On the lattice, corrections might spoil the picture for sufficiently separated instantons. The state which minimizes Eq. (13) might have different weights for different well-separated structures. A signal that this is actually happening can be obtained from the hierarchy of low-

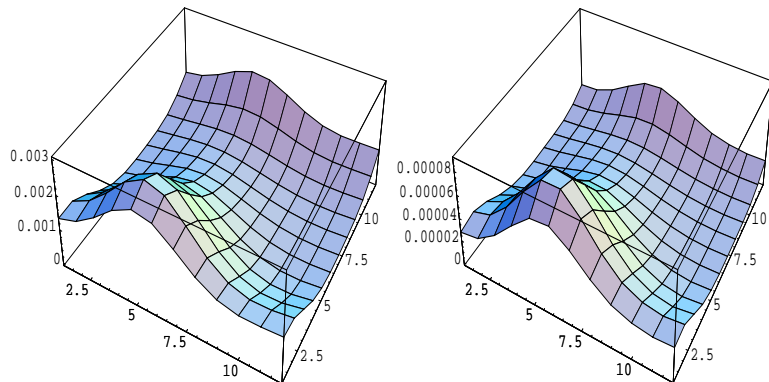


Figure 4: *Action (left) and chiral (right) densities for the $Q = 2$ configuration; Both given for y - z plane.*

lying eigenvalues of M . A set of small eigenvalues separated by a large gap from higher ones is a clear indication of this situation. The supersymmetric solution we are looking for is then a linear combination of the states constructed from the eigenstates pertaining to the minimal eigenvalues of M . For sufficiently smooth configurations the correct weights can be constrained since the contribution to the total action and topological charge of each separated structure must be in rational fraction of the total.

We have looked at several $Q = 2$ configurations that contained well separated (anti) self-dual lumps. In one case we found precisely the scenario described above, while for other configurations the numerical method described in Section 3.1 projected directly onto the supersymmetric solution of Eq. (8).

So far we have checked that our numerical method of projecting onto the supersymmetric zero-mode Eq. (8) works well for (anti) self-dual fields. In the next subsection we will consider a more complicated structure which no longer is a solution of the classical euclidean equations of motion.

4.2 Other Smooth Configurations

Our next step will be to consider the case of smooth configurations which are not solutions of the classical equations of motion. For that purpose we study a $Q = 0$ configuration consisting of an instanton and an anti-instanton, each carrying charge $|Q| = 1$. Note that in this case we do not have exact zero modes in the continuum. However, we expect that if the instantons are sufficiently separated, so that their overlap is small, the zero-modes pertaining to each instanton will give rise to *near-zero* modes in the spectrum of $(\gamma_5 D_W)^2$. In our $Q = 0$ instanton anti-instanton pair case, we should find eight near-zero modes stemming from the four zero-modes of an isolated instanton. Furthermore, we expect to be able to identify within the space of *near-zero* modes one state in each chirality sector arising from the supersymmetric zero-modes Eq. (8) of the

instanton and anti-instanton separately.

$$Q = +1 - 1 = 0, \mathbf{m}=\mathbf{k}=\{000\}$$

To produce a smooth $Q = 0$ lattice configuration consisting of an instanton anti-instanton pair, we glued along the time direction the previously mentioned $Q = -1$ configuration to a time reflected copy of itself. The resulting configuration has an increased action density along the plane of gluing. We then applied several cooling steps to diminish the action. The resulting configuration (see Figure 5) has an action density which looks indeed like a superposition of an instanton and an anti-instanton. For this configuration we computed the twenty

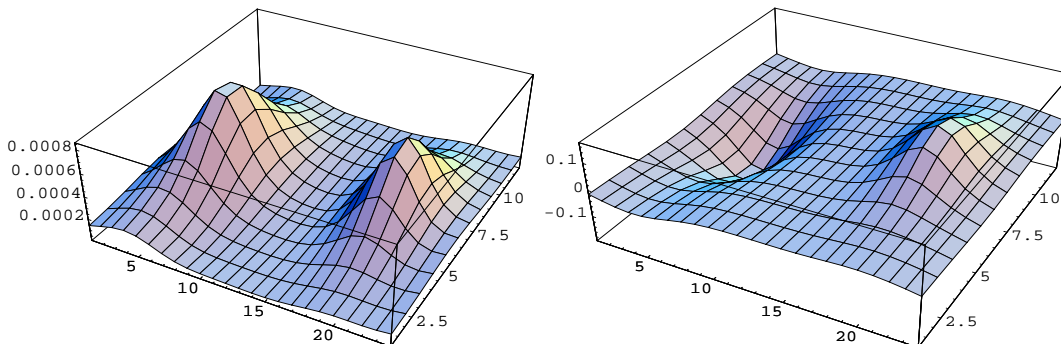


Figure 5: *Action density (left) and charge density (right) of the glued $Q=0$ configuration.*

lowest-lying eigenmodes of the operator $(\gamma_5 D_W)^2$ at $r = 0.3$ (see Table 6). We

Eigenvalue	$\langle \phi, \gamma_5 \phi \rangle$	Eigenvalue	$\langle \phi, \gamma_5 \phi \rangle$
$\lambda_1=2.50 * 10^{-3}$	-0.725	$\lambda_{11}=1.32 * 10^{-2}$	0.119
$\lambda_3=3.42 * 10^{-3}$	0.337	$\lambda_{13}=3.61 * 10^{-2}$	$-6.54 * 10^{-2}$
$\lambda_5=4.94 * 10^{-3}$	-0.439	$\lambda_{15}=3.66 * 10^{-2}$	$6.70 * 10^{-2}$
$\lambda_7=6.44 * 10^{-3}$	0.804	$\lambda_{17}=5.20 * 10^{-2}$	$-4.67 * 10^{-2}$
$\lambda_9=1.195 * 10^{-2}$	-0.117	$\lambda_{19}=5.26 * 10^{-2}$	$5.00 * 10^{-2}$

Table 6: *Lowest lying eigenvalues of the operator $(\gamma_5 D_W)^2$ and chiralities of the respective eigenstates, for the instanton-antiinstanton configuration.*

see that in our case no clear gap in the eigenvalue spectrum can be identified. The zero-modes of the original $Q = -1$ configuration (see Table 3) have been lifted to near-zero modes. Given the large separation of the instanton and anti-instanton, we expect that the near-zero modes associated to the supersymmetric states lie within the eight lowest-lying modes. Hence, we computed the observables S_{\pm} by minimizing expression (13) within this space. These quantities are

shown in Figure (6). We see that they reproduce nicely the shape of the self-dual and the anti self-dual parts of the action density respectively. We recalculated S_{\pm} within the full space of twenty low-lying eigenmodes. Once more, our results were found to be stable.

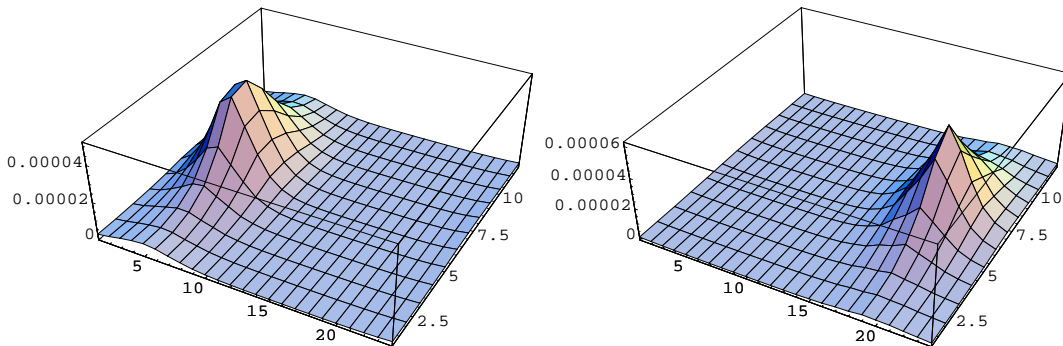


Figure 6: Chiral density $(\Psi_R^\dagger)^\dagger \Psi_R^\dagger$ (right) and $(\Psi_L^\dagger)^\dagger \Psi_L^\dagger$ (left), for our instanton-anti-instanton configuration.

4.3 Heated Configurations

We now want to go one step further and investigate the efficiency of our method in the presence of quantum fluctuations. As explained in the introduction this amounts to the consideration of rough configurations. Optimally we would like to add quantum fluctuations without distorting the long-wavelength topological structure of the configuration, so that we can compare our observable fields S_{\pm} with the mentioned structure. To achieve this goal we use the following method. We begin with a classical anti self-dual configuration for definiteness. Then we apply a given number of heat-bath steps with a certain value of β . The local nature of the heat-bath algorithm [47] guarantees that the high-momentum modes will thermalize faster than the low momentum modes. Based on results obtained in other contexts [14] we conclude that a total of ten to twenty heating steps should be enough for this purpose. The value of β determines the typical size of the quantum fluctuations ($\sim 1/\sqrt{\beta}$), as well as the effect of non-linearities. Thus, we started by considering a very high value of β , namely $\beta = 22$. This introduces gaussian perturbations (up to gauge equivalence). As initial configuration, we chose the second one in Table 1. We applied a total of twenty heating steps to it. After each heating step, we calculated the sixteen lowest-lying eigenstates of $(\gamma_5 D_W)^2$ at $r = 0.3$. From them, we calculated the observable S_- according to the procedure outlined in Section 3.2. The results obtained confirm the good behavior of S_- with respect to quantum fluctuations. At each heating step β , S_- resembled closely the shape of the starting configuration. This contrasts with the evaluation of the action density itself (or its anti-self-dual part) which is dominated by noise, masking completely the initial topological

structure. Indeed, the action density after heating is two orders of magnitude higher than the action density of the original field.

Then we considered two smaller values of β , $\beta = 5$ and $\beta = 2.57$. The latter lies in the relevant scaling region of Monte-Carlo simulations. As we lower β the fluctuations have a larger size and we depart from the gaussian situation, in which analytical control is still possible. Furthermore, the probability of generating typical lattice artifact effects, like the dislocations [48, 49], increases. These structures can contribute sizably to the topological charge for some lattice definitions of the quantity. This effect on the topology can also show up in the Dirac spectrum. It has been shown in $SU(2)$ gauge theory that, with the plaquette action, dislocations appear quite frequently, but that they disappear after only a few cooling steps [49, 50]. For this reason we introduce a small number of cooling steps (3) on the heated configuration and proceed with our method on this slightly cooled configuration. The use of a fixed and small number of cooling steps might be acceptable if we can show that the results are insensitive to the details of their implementation.

For that purpose we have also used APE-smearing [13] (see Section 3.3) instead of cooling to smoothen the heated configurations. We have chosen $N = 8$ and $c = 0.45$ as smearing parameters, so that the effective smearing radius and the number of cooling steps are of the same magnitude. As we will show below both methods do not only give consistent results, but lead to values of S_{\pm} that are strikingly similar.

4.3.1 Updating at $\beta = 5.00$

Again we started with the $Q = -1$ configuration appearing as example two in Subsection 4.1, with action density displayed in Figure 2. At $\beta = 5.00$ we subjected the configuration to twenty heating steps. Every fifth step we produced a (three times) cooled or a ($N = 8$ $c = 0.45$) smeared configuration. The corresponding values of of the topological charge and the action can be found in Table 7. As we can see no extra charge seems to have been created during heating.

heating	$S/(8\pi^2)$	Q_L	S_{cool}	$Q_{L,cool}$	S_{smear}	$Q_{L,smear}$
0	1.02	-0.90	–	–	–	–
5	991.8	-0.56	6.5	-0.87	5.0	-0.87
10	993.9	-0.41	6.6	-0.86	5.2	-0.84
15	990.3	-1.02	6.6	-0.86	5.1	-0.86
20	993.9	-0.60	6.5	-0.86	5.0	-0.86

Table 7: Values of the action S (divided by $8\pi^2$) and topological charge (field theoretic) of the heated (at $\beta = 5.00$), cooled (3 times) or smeared configurations on a 12^4 lattice.

For each of the cited configurations the sixteen lowest lying eigenmodes of the

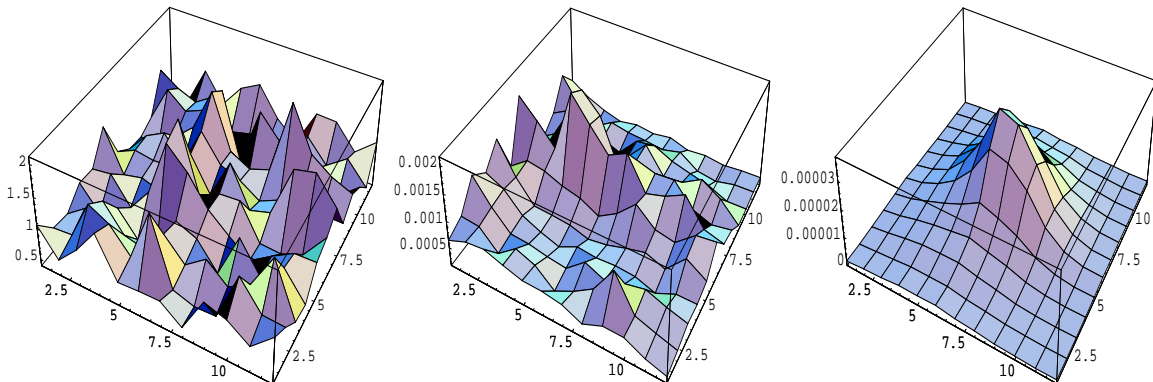


Figure 7: *Action density of the heated configuration after 5 heating steps (left) with $\beta = 5.00$, and after applying 3 cooling steps to the previous one(middle). The right figure is the chiral density $\Psi_R^\dagger \Psi_R$ obtained from the near zero-modes of the cooled configuration.*

operator $(\gamma_5 D_W)^2$ have been calculated at $r = 0.3$. We then determined S_\pm by applying the minimization of expression (13) in this sixteen dimensional subspace of eigenmodes. The results for 5 and 20 heating steps can be found in Figure (7, 8).

We observe that in all cases the shape of S_- resembles fairly well the action density of the original configuration. After twenty heating steps the qualitative agreement is still quite good. Similar results are obtained for the smeared configurations. Hence, we conclude that our results are independent of the method used — smearing or cooling — to remove the lattice artefacts.

It is interesting to point out that the heating process does not seem to have changed the long wavelength structure of the initial configuration. This is due to the large value of β and the small number of heating steps. In the next subsection we will see that the situation changes for smaller values of β .

4.3.2 Updating at $\beta = 2.57$

Let us now turn to the $\beta = 2.57$ case, which is the most interesting case in understanding the behavior of our observables previous to their use for Monte Carlo generated configurations. Our procedure is identical to the previous case. Results for the topological charge and the action can be found in Table 8.

At this value of β we expect that, after a sufficient number of heating steps are applied, the configuration will have modified the long-wavelength structure of the initial configuration. It is then unclear what the shape of S_\pm has to be. Notice, however, that the value of Q_L after cooling indicates that no extra overall charge has been created during the updating. This does not exclude that a number of instanton-anti-instanton pairs have been created in this process.

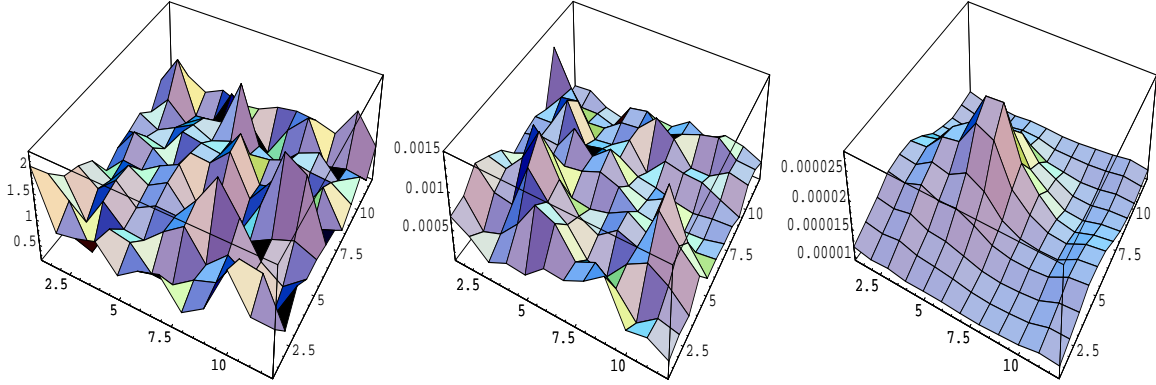


Figure 8: *The same quantities as in the previous figure but after 20 heating steps at $\beta = 5.00$.*

heating	$S/(8\pi^2)$	Q_L	S_{cool}	$Q_{L,cool}$	S_{smear}	$Q_{L,smear}$
0	1.02	-0.90	—	—	—	—
5	2074.7	-0.96	16.6	-0.88	14.56	-0.88
10	2119.7	0.47	21.8	-0.84	21.48	-0.84
15	2110.7	1.38	23.5	-0.89	23.46	-0.86
20	2110.2	-0.84	22.7	-0.91	22.85	-1.00

Table 8: *Action and topological charge (field theoretic) of the heated (at $\beta = 2.57$), cooled and smeared configurations on a 12^4 lattice.*

As in the previous case, we compute the fields S_{\pm} in terms of the low-lying eigenmodes of the operator $(\gamma_5 D_W)^2$ after 5 and 20 heating steps. Results are shown in Figs. (9 - 10).

We observe, that after 5 heating steps one can still recognize in S_- the structure of the original anti-instanton. After 20 heating steps, however, we can see a richer structure emerging. The main peak of the original instanton is still present, but two additional lumps in this plane seem to have been created during the heating process. Since there seems to be no net creation of topological charge, we expect to find two structures in S_+ corresponding to positively charged lumps. The result is shown Fig. 11, and we can clearly identify two isolated structures, which we associate to two instantons that have been created during the heating process.

Let us compare the chiral densities obtained from the cooled configurations to the ones that result by carrying out the same procedure on the smeared configurations. The corresponding chiral densities for the heated and successively

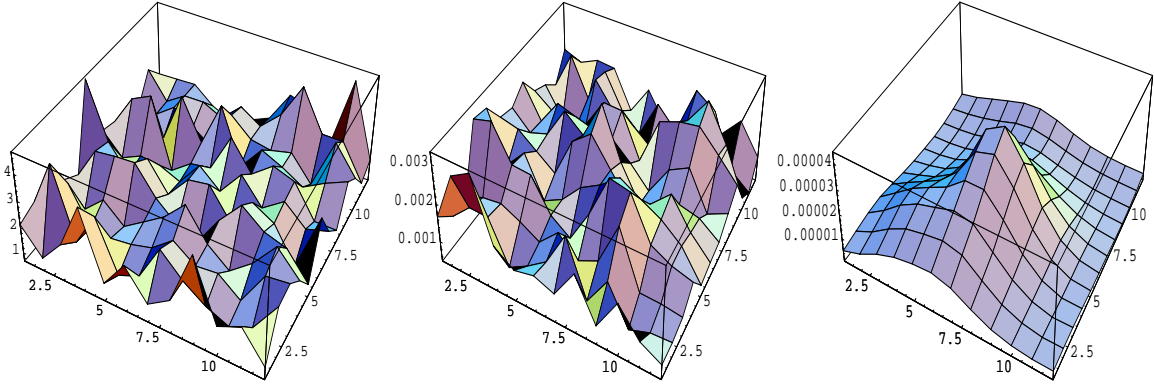


Figure 9: *The same as Fig. 7 but after 5 heating steps at $\beta = 2.57$*

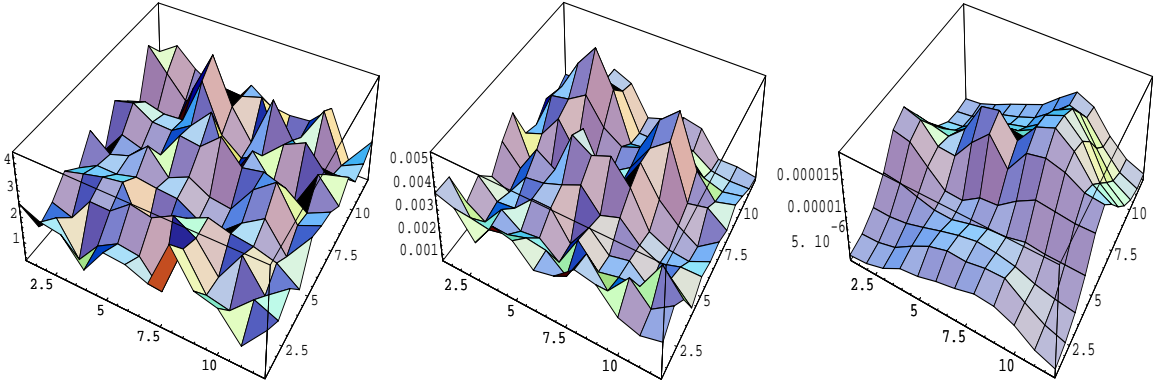


Figure 10: *The same as Fig. 8 for $\beta = 2.57$*

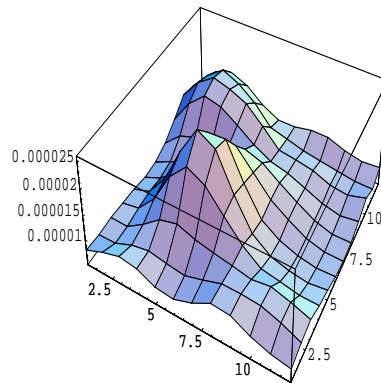


Figure 11: *Chiral density $\Psi_L^\dagger \Psi_L$ of minimized linear combination obtained from the cooled configuration at $\beta = 2.57$.*

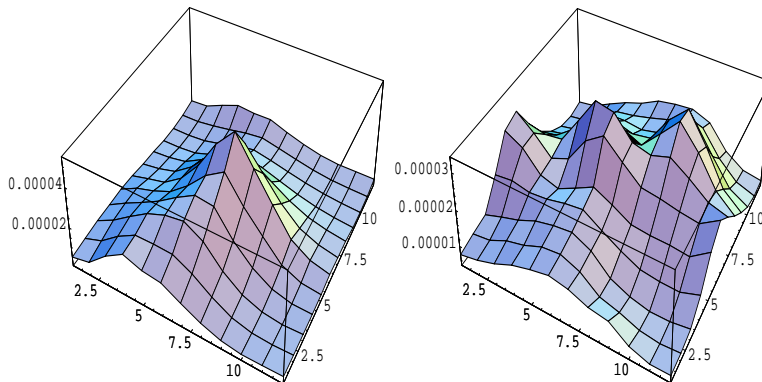


Figure 12: Chiral density $\Psi_R^\dagger \Psi_R$ (left) of minimized linear combination obtained from the smeared configurations after 5 heating steps (left) and after 20 heating steps (right).

smeared configurations can be found in Figure 12. These figures when compared to the chiral densities obtained from the cooled configurations are strikingly similar. Accordingly we conclude that smearing as well as cooling disposes of the lattice artefacts in the same manner and that the same underlying structure is revealed by our procedure.

5 Conclusions

In this work we have proposed a new tool to investigate the vacuum structure of gauge field theory. It is in the spirit of using fermionic modes as probes of gauge field structure. However, we make use of fermions in the adjoint representation. For gauge fields which are exact solutions of the euclidean equations of motion, Supersymmetry gives rise to a direct connection between the structure of some zero-modes and the gauge field strength. In the presence of quantum fluctuations one can use this idea to construct observables S_\pm which reflect the underlying self-dual and anti-self dual components and are better behaved in the ultraviolet.

In this paper our main goal has been to present the ideas and to test its ability to reconstruct the underlying gauge field structure in an increasingly complex but controlled situation. Thus, we have first analyzed the case of smooth self-dual gauge fields and shown that indeed our method is capable of extracting the supersymmetric zero-modes that match the shape of the action density. Next we have studied the case of smooth, non-self-dual configurations. Finally we have analyzed configurations having controlled quantum fluctuations. This was achieved by applying a number of heat-bath sweeps to an initially self-dual configuration. We used the number of heating steps and the value of β to monitor the size of quantum fluctuations and their local nature. For

small enough number of heating steps or large enough β , the chiral density of the linear combination of low-lying eigenmodes that best approximates the supersymmetric mode, reproduces the action density of the underlying anti-instanton on which heating was performed. This contrasts with the value of the action density itself, which has little resemblance to the initial structure.

For $\beta = 2.57$ we have found that after 20 heating steps, next to the original anti-instanton, additional structures have developed during the heating process. We interpret them as instanton anti-instanton pairs that have been created during updating. Although we had to apply three cooling steps to the configuration before analyzing the zero-modes, we argue that this operation has not distorted the underlying structure that we are looking for. In support of this claim we showed that the shape obtained is remarkably similar to the one gotten from the Ape-smear configuration instead.

The analysis presented in this paper serves as a test of the usefulness of our construction in being able to unravel, for a given gauge field configuration, the underlying topological structure masked by short wavelength fluctuations. The next step should be that of addressing Monte Carlo generated configurations directly. For that purpose it is presumably essential to use a lattice Dirac operator, such as Neuberger operator, which preserves an exact notion of chirality.

We hope our work provides a new tool that can be used, by itself or in conjunction with other methods, to study the topological structures present in the QCD vacuum in the spirit of the works mentioned in the introduction [24–29, 31–34, 37, 51–53].

Acknowledgements

We thank Margarita García Pérez for interesting discussions, suggestions and a critical reading of the manuscript.

6 Appendix

In this Appendix we list the conventions and definitions that were used throughout this work.

Generalities

The number of colors has been denoted by N . For the specific numerical calculations we work in the adjoint representation of $SU(2)$, hence $N = 2$. Color in the adjoint representation is labeled by Latin lower indices of the form $a, b, c, \dots = 1, \dots, N^2 - 1$.

Greek lower case letters from the beginning of the alphabet such as $\alpha, \beta, \dots = 1, \dots, 4$ label the spinorial indices. Greek lower case letters from the middle of the alphabet such as $\mu, \nu, \rho, \sigma, \dots = 0, \dots, 3$ denote Lorentz space-time components (in Euclidean space-time).

SU(N) group

The generators of the Lie-algebra $su(N)$ of the gauge group $SU(N)$ in the fundamental representation are denoted by T^a with $a \in \{1, \dots, N^2 - 1\}$ and are given by $N \times N$ matrices. Their commutation relations read

$$[T^a, T^b] = if^{abc}T^c. \quad (17)$$

where f^{abc} are the structure constants of the group. These generators are normalized according to

$$\text{Tr}[T^a T^b] = \frac{1}{2}\delta^{ab}.$$

For a given group element $g \in SU(N)$, $U(g)$ will denote its corresponding matrix in the fundamental representation and $V(g)$ in the adjoint representation. The matrix elements of the latter can be expressed in terms of $U(g)$ as follows

$$V(g)^{ab} = \frac{1}{2}\text{Tr}[U^\dagger(g)T^a U(g)T^b]. \quad (18)$$

Pauli and Euclidean Dirac matrices

The symbol τ^a denotes the Pauli matrices:

$$\tau_1 = \begin{pmatrix} 0 & 1 \\ 1 & 0 \end{pmatrix}, \quad \tau_2 = \begin{pmatrix} 0 & -i \\ i & 0 \end{pmatrix}, \quad \tau_3 = \begin{pmatrix} 1 & 0 \\ 0 & -1 \end{pmatrix}. \quad (19)$$

We also define the quaternionic basis $\sigma_\mu = (\mathbb{1}, -i\vec{\tau})$, $\bar{\sigma}_\mu = \sigma_\mu^\dagger = (\mathbb{1}, i\vec{\tau})$. The hermitian Dirac matrices γ_μ in the Weyl representation in Euclidean space-time are given in terms of the previous matrices by

$$\gamma_\mu = \begin{pmatrix} 0 & \sigma_\mu \\ \bar{\sigma}_\mu & 0 \end{pmatrix}. \quad (20)$$

We also define the following matrices

$$\gamma_5 = \gamma_1\gamma_2\gamma_3\gamma_0 = \begin{pmatrix} \mathbb{1} & 0 \\ 0 & -\mathbb{1} \end{pmatrix}, \quad C = \gamma_0\gamma_2 = \begin{pmatrix} i\tau_2 & 0 \\ 0 & -i\tau_2 \end{pmatrix}, \quad (21)$$

The charge conjugation matrix C fulfills the following relations

$$C^{-1} = -C = C^T, \quad \gamma_\mu^T = -C^{-1}\gamma_\mu C, \quad \gamma_5 = C^{-1}\gamma_5 C. \quad (22)$$

The eigenstates of γ_5 with eigenvalue 1 are called positive chirality or left-handed spinors. Conversely, negative chirality or right-handed spinors apply for the eigenstates of eigenvalue -1 . Any spinor can be decomposed into a sum of a right-handed and a left-handed spinor $\psi = \psi_R + \psi_L$, where the latter can be obtained from ψ using the projection operators $P_\pm = (\mathbb{1} \pm \gamma_5)/2$.

For the antisymmetric tensor $\epsilon_{\mu\nu\rho\sigma}$ we take the sign convention $\epsilon_{0123} = 1$.

References

- [1] A.A. Belavin, A.M. Polyakov, A.S. Schwartz, and Y.S. Tyupkin. *Phys. Lett.*, B 59:85, 1975.
- [2] G. 't Hooft. *Phys. Rev. Lett.*, 37:8, 1976.
- [3] E. V. Shuryak. *Nucl. Phys.*, B 198:83.
- [4] D. I. Diakonov and V. Y. Petrov. *Nucl. Phys.*, B 245:259, 1984.
- [5] T. Schäfer and E. Shuryak. *Rev. Mod. Phys.*, 70:323, 1998.
- [6] T. Banks and A. Casher. *Nucl. Phys.*, B 169:103, 1980.
- [7] D. I. Diakonov and V. Y. Petrov. *Nucl. Phys.*, B 272:457, 1986.
- [8] A. González-Arroyo and P. Martínez. *Nucl. Phys.*, B 459:737, 1996.
- [9] A. González-Arroyo and Y. Simonov. *Nucl. Phys.*, B 460:424, 1996.
- [10] M. Teper. *Phys. Lett.*, B 171:81,86, 1986.
- [11] E. M. Ilgenfritz, M. L. Laursen, G. Schierholz, M. Muller-Preussker, and H. Schiller. *Nucl. Phys.*, B 268:693, 1986.
- [12] P. de Forcrand, M. García-Pérez, and I. O. Stamatescu. *Nucl. Phys.*, B 413:535, 1994.
- [13] M. Albanese, F. Costantini, G. Fiorentini, F. Flore, M. Lombardo, R. Tripiccion, and P. Bacilieri. *Phys. Lett.*, B 192:163, 1987.
- [14] B. Allés, M. Campostrini, A. DiGiacomo, Y. Gündüç, and E. Vicari. *Phys. Rev.*, D 48:2284, 1993.

- [15] B. Allés, M. D’Elia, A. DiGiacomo, and R. Kirchner. *Phys. Rev.*, D 58:114506, 1998.
- [16] A. Hasenfratz and C. Nieter, *Phys. Lett.* B 439:366, 1998.
- [17] T. DeGrand, A. Hasenfratz and T. G. Kovacs, *Nucl. Phys.* B 520:301, 1998.
- [18] S. Hands and M. Teper. *Nucl. Phys.*, B 347:819, 1990.
- [19] D. B. Kaplan. *Phys. Lett.*, B 288:324, 1992.
- [20] Y. Shamir. *Nucl. Phys.*, B 406:90, 1993.
- [21] Y. Shamir and V. Furman. *Nucl. Phys.*, B 439:54, 1995.
- [22] H. Neuberger. *Phys. Lett.*, B 417:141, 1998.
- [23] H. Neuberger. *Phys. Lett.*, B 427:353, 1998.
- [24] T. DeGrand and A. Hasenfratz. *Phys. Rev.*, D 64:034512, 2001.
- [25] T. DeGrand and A. Hasenfratz. *Phys. Rev.*, D 65:014503, 2002.
- [26] C. Gattringer, M. Göckeler, P. Rakow, S. Schaefer, and A. Schäfer. *Nucl. Phys.*, B 618:205, 2001.
- [27] R. Edwards and U. Heller. *Phys. Rev.*, D 65:014505, 2002.
- [28] T. Blum, N. Christ, C. Cristian, C. Dawson, X. Liao, G. Liu, R. Mawhinney, L. Wu, and Y. Zhestkov. *Phys. Rev.*, D 65:014504, 2002.
- [29] I. Horváth, S. Dong, T. Draper, N. Isgur, F. Lee, K. Liu, J. McCune, H. Thacker, and J. Zhang. *Phys. Rev.*, D 66:034501, 2002.
- [30] N. Cundy, M. Teper, and U. Wenger. *Phys. Rev.*, D 66:094505, 2002.
- [31] I. Horvath *et al.*. *Phys. Rev.* D 68:114505, 2003.
- [32] I. Horvath. *Nucl. Phys.* B 710:464, 2005; Erratum-ibid. B 714:175, 2005.
- [33] I. Horvath *et al.*. *Phys. Lett.* B 612:21, 2005.
- [34] I. Hip, T. Lippert, H. Neff, K. Schilling, and W. Schroers. *Phys. Rev.*, D 65:014506, 2002.
- [35] C. Gattringer. *Phys. Rev. Lett.*, 88:221601, 2002.
- [36] I. Horváth, S. Dong, T. Draper, F. Lee, K. Liu, H. Thacker, and J. Zhang. *Phys. Rev.*, D 67:011501, 2003.
- [37] I. Horváth, N. Isgur, J. McCune, and H. B. Thacker. *Phys. Rev.*, D 65:014502, 2002.

- [38] G. 't Hooft. *Comm. Math. Phys.*, 81:267, 1981.
- [39] P. van Baal. *Comm. Math. Phys.*, 85:529, 1982.
- [40] S. Donaldson and P. Kronheimer The geometry of four-manifolds, *The geometry of four-manifolds*, Oxford UP, 1990.
- [41] S. Chada, A. D'Adda, P. DiVecchia, and F. Nicodemi. *Phys. Lett.*, 67B:103, 1977.
- [42] R. Jackiw and C. Rebbi. *Phys. Rev.*, D 16:1052, 1977.
- [43] M.F. Atiyah, N.J. Hitchin, V.G. Drinfeld, and Y. Manin. *Phys. Lett.*, A 65:185, 1978.
- [44] T. Kalkreuter and H. Simma. *Comput. Phys. Commun.*, 93:33, 1996.
- [45] D.C. Sorensen. *SIAM*, 13(1):357, 1992. The software is publicly available at <http://www.caam.rice.edu/software/ARPACK/>.
- [46] P. DiVecchia, K. Fabricius, G.C. Rossi, and G. Veneziano. *Nucl. Phys.*, B 192:392, 1981.
- [47] M. Creutz. *Phys. Rev.*, D 21:2308, 1980.
- [48] M. Lüscher. *Nucl. Phys.*, B 200:61, 1982.
- [49] D. J. R. Pugh and M. Teper. *Phys. Lett.*, B 218:326, 1989.
- [50] D. J. R. Pugh and M. Teper. *Phys. Lett.*, B 224:159, 1989.
- [51] C. Gattringer, M. Göckeler, P. Rakow, S. Schaefer, and A. Schäfer. *Nucl. Phys.*, B 617:101, 2001.
- [52] C. Gattringer and S. Schaefer. *Nucl. Phys.* B 654:30, 2003.
- [53] C. Gattringer and R. Pullirsch. *Phys. Rev.* D 69:094510, 2004.